



# Electrosynthesis of gradient TiO<sub>2</sub> nanotubes and rapid screening using scanning photoelectrochemical microscopy

Florian Gelb, Yu-Chien Chueh, Neso Sojic, Valérie Keller, Dodzi Zigah,  
Thomas Cottineau

## ► To cite this version:

Florian Gelb, Yu-Chien Chueh, Neso Sojic, Valérie Keller, Dodzi Zigah, et al.. Electrosynthesis of gradient TiO<sub>2</sub> nanotubes and rapid screening using scanning photoelectrochemical microscopy. Sustainable Energy & Fuels, 2020, 4 (3), pp.1099-1104. 10.1039/C9SE00895K . hal-03093977

**HAL Id: hal-03093977**

**<https://hal.science/hal-03093977>**

Submitted on 7 Jan 2021

**HAL** is a multi-disciplinary open access archive for the deposit and dissemination of scientific research documents, whether they are published or not. The documents may come from teaching and research institutions in France or abroad, or from public or private research centers.

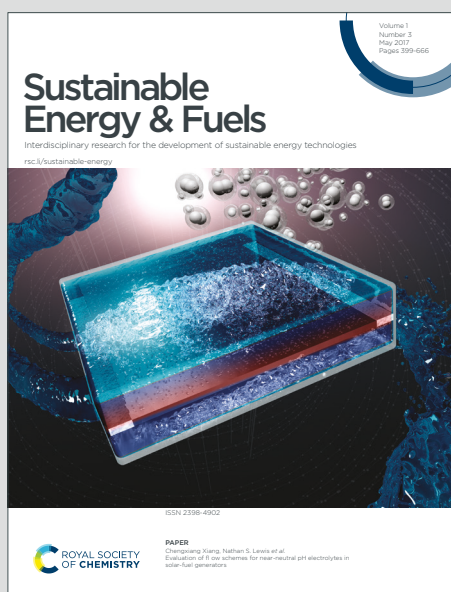
L'archive ouverte pluridisciplinaire **HAL**, est destinée au dépôt et à la diffusion de documents scientifiques de niveau recherche, publiés ou non, émanant des établissements d'enseignement et de recherche français ou étrangers, des laboratoires publics ou privés.

# Sustainable Energy & Fuels

Interdisciplinary research for the development of sustainable energy technologies

Accepted Manuscript

This article can be cited before page numbers have been issued, to do this please use: F. Gelb, Y. Chueh, N. Sojic, V. KELLER, D. Zigah and T. Cottineau, *Sustainable Energy Fuels*, 2020, DOI: 10.1039/C9SE00895K.



This is an Accepted Manuscript, which has been through the Royal Society of Chemistry peer review process and has been accepted for publication.

Accepted Manuscripts are published online shortly after acceptance, before technical editing, formatting and proof reading. Using this free service, authors can make their results available to the community, in citable form, before we publish the edited article. We will replace this Accepted Manuscript with the edited and formatted Advance Article as soon as it is available.

You can find more information about Accepted Manuscripts in the [Information for Authors](#).

Please note that technical editing may introduce minor changes to the text and/or graphics, which may alter content. The journal's standard [Terms & Conditions](#) and the [Ethical guidelines](#) still apply. In no event shall the Royal Society of Chemistry be held responsible for any errors or omissions in this Accepted Manuscript or any consequences arising from the use of any information it contains.

## Electrosynthesis of gradient TiO<sub>2</sub> nanotubes and rapid screening using Scanning PhotoElectroChemical Microscopy

Received 00th January 20xx,  
Accepted 00th January 20xx

Florian Gelb,<sup>a</sup> Yu-Chien Chueh,<sup>b</sup> Neso Sojic,<sup>b</sup> Valérie Keller,<sup>a</sup> Dodzi Zigah<sup>b</sup> and Thomas Cottineau<sup>\*a</sup>

DOI: 10.1039/x0xx00000x

Herein, we report a new approach that allows a fast investigation of the influence of the thickness of a TiO<sub>2</sub> photoelectrochemical film. For this we developed a simple anodization method that allows to grow, in one step, on a single titanium electrode, aligned TiO<sub>2</sub> nanotubes with length changing gradually between 0 to 10  $\mu\text{m}$ . We were able to tune the length of the tubes by controlling the immersion time within the electrolyte during the synthesis. The change of the nanotube length over the entire surface of the electrode requires local probes to measure their properties. Therefore, in order to determine the optimal length of the nanotubes for photoelectrochemical application, the response of these electrodes was locally analysed using Scanning PhotoElectroChemical Microscopy.

### Introduction

Since several years there is a strong interest in light energy conversion motivated by the huge potential of renewable and clean energy provided by the sun combined to the urge related to climate change and to the diminution of fossil fuel resources easily accessible at low cost.<sup>1</sup> New concepts are investigated with the objectives to decrease the price and to improve the conversion efficiency such as dye sensitized solar cells (DSSC) or more recently cells based on perovskite absorber are promising PV systems.<sup>2</sup> Alternatively Photo-electrochemical cells (PEC) would pave the way to the direct production of solar fuel from sunlight.<sup>3,4</sup> Several of these new concepts relies on thick porous semiconducting films that are responsible of the charge carrier transport (for DSSC) and also for light absorption (PEC).<sup>5,6</sup> It is necessary to find the optimal thickness of these films in order to manage the light and charge carrier transportation in the cell.<sup>7–9</sup> This is particularly true for the case of tandem PEC cell in which two semi conductors

absorbing in two different spectral domains would be associated.<sup>10</sup> The large band gap semiconductor would be in that case in front irradiation configuration and a compromise should be found on the film thickness. Indeed, if a thick layer of photoactive material maximizes the light absorption (mainly at the top of the film), it can result in a reduced photo-generated charge carrier collection at the back contact due to their probability of recombination on long distance.

In this context, the development of rapid screening methods of the film performances as a function of their thickness should be developed. Achieving such measurements requires two conditions: The first requirement is to obtain electrodes with a variable and well controlled thickness of photoactive material. The change of the thickness must not have any impact on the morphology or other properties of the material such as its conductivity or its composition. The second requirement is to have a system that can achieve local PEC analysis with the highest resolution possible which is mainly related to the irradiation area.

So far the large majority of rapid screening experiments were used to determine the optimal composition of ternary oxides.<sup>11,12</sup> For instance, an ambitious distributed combinatorial outreach program was conducted a few years ago using inkjet printing of semi-conductor with variable composition on conductive glass substrates.<sup>13</sup> The most relevant example we found concerning rapid PEC screening to study the influence of geometrical parameters on a single electrode, was done by Loget et al.<sup>14</sup> They used a bipolar anodization method to grow titanium dioxide nanotubes (TiO<sub>2</sub>-NTs) with variable length on a single electrode. The bipolar anodization method was also employed to synthesize gradient of TiO<sub>2</sub>-NTs for photo-catalytic and biomedical applications.<sup>15,16</sup> Nevertheless, considering the formation mechanism of anodic TiO<sub>2</sub>-NTs,<sup>17</sup> the potential variation along the Ti foil in bipolar anodization induces a change of the NTs length but it also changes the diameter and the wall thickness of the tubes. Consequently, the apparent density of TiO<sub>2</sub> in the film will change and the mean free path of light will not be homogeneous for the whole electrode. Furthermore, during the bipolar synthesis, it is not possible to determine the charge transferred at each position of the electrode. The knowledge of this value is important since it can be directly related to the

<sup>a</sup> CNRS, Univ. Strasbourg, Institut de Chimie et Procédés pour l'Energie, l'Environnement et la Santé, UMR 7515, 25 rue Becquerel, 67087 Strasbourg, France.

<sup>b</sup> Univ. Bordeaux, CNRS, Bordeaux INP, Institut des Sciences Moleculaires, UMR5255, 16 Avenue Pey-Berland, 33400 Talence, France

\* Corresponding author: [cottineau@unistra.fr](mailto:cottineau@unistra.fr)

Electronic Supplementary Information (ESI) available: Detailed experimental parameters; Optical image and full set of SEM images for the VLTE sample; CV and EQE of reference TiO<sub>2</sub>-NTs Electrode; XRD and stability tests of VLTE sample; anodization curve of the second VLTE sample. See DOI: 10.1039/x0xx00000x

quantity of TiO<sub>2</sub> electrochemically formed during the anodization of the titanium foil. Furthermore, in all the studies mentioned above, the light source used had a spot diameter larger than 1 mm, which limits the accuracy on the local photocurrent determination.

Scanning PhotoElectroChemical Microscopy (SPECM) is a scanning probe technique that uses an optical fiber (or an optoelectrode) as a probe to analyze a surface locally.<sup>18–20</sup> Unlike conventional photoelectrochemical measurements, which give a global response of the surface, in SPECM a local response is obtained. In this configuration the spatial resolution is determined by the illuminated area. The use of an optical fiber allows the photoelectrochemical reaction to be triggered only where the surface is illuminated.<sup>21–23</sup> The small aperture of the optical fiber and the short distance between the fiber and the sample result in a small spot size of around 200 µm. Therefore, SPECM is a technique of choice to study an inhomogeneous surface or to screen different materials present on the same substrate. As an example, it was used to determine the optimal Zn doping of WO<sub>3</sub> on material spots deposited on a single electrode<sup>24</sup> and also to show that addition of Ag improves the behaviour of Fe<sub>2</sub>O<sub>3</sub> by screening micrometer spots with different composition.<sup>25</sup> In our case, we were able, with the SPECM, to make a rapid screening, with a high resolution, of the nanotubes properties.

In the present work, we developed a new method to synthesize anodic TiO<sub>2</sub>-NTs with a changing length on a single electrode (here after named VLTE for Variable Length TiO<sub>2</sub>-NTs Electrode). This simple method allows making an electrode fully covered with these NTs which have an increasing length in one direction of the film. These model electrodes with variable nanotube length were then tested with SPECM in order to determine to optimal TiO<sub>2</sub>-NTs film thickness for their use as photoanode for water splitting.

## Variable length TiO<sub>2</sub>-NTs electrode synthesis

To achieve the growth of TiO<sub>2</sub>-NTs with a gradual length on a single electrode, we developed a simple method based on the control of the exposure time of the titanium to the electrolyte. Such approach was attempted earlier but in a configuration in which both the electrolyte exposure time and the applied potential were changed.<sup>26</sup> For this reason and also due to the use of aqueous based electrolyte, mainly the diameter of the NTs was changed and the length only increased from 300 to 500 nm.

In our case for growing NTs with different lengths, a titanium foil and the platinum electrode are placed vertically in a Teflon cell as schematically represented in **figure 1**. At the beginning of the synthesis, both electrodes are immersed in an ethylene glycol based electrolyte which is then slowly removed from the cell by a peristaltic pump. As the level of electrolyte goes down progressively, an increasing part of the titanium is not anymore in contact with the electrolyte and the nanotube growth is inhibited in that area. After the synthesis, the electrode is then carefully rinsed with deionized water and dry under nitrogen flux and annealed at 500°C under air for 4h.

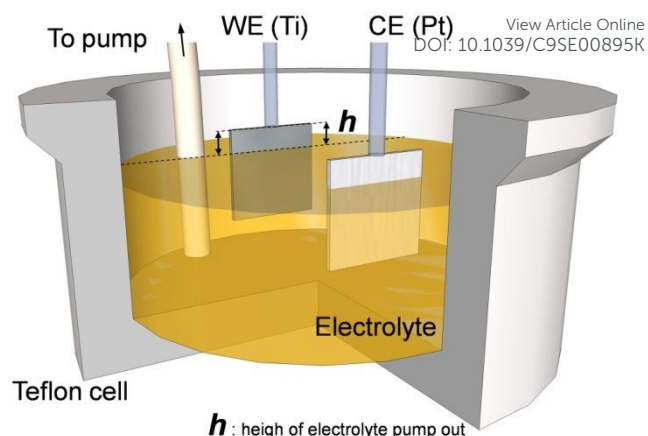
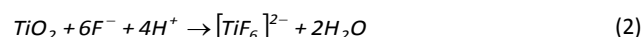
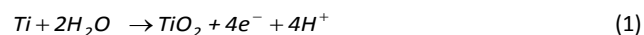


Figure 1 : Schematic principle of VLTE synthesis by electrolyte pumping.

(detailed synthesis conditions are given in Electronic Supplementary Information ESI)

After the experiment, the electrode exhibits horizontal iridescences which are a first indication of the change of the thickness of the TiO<sub>2</sub>-NTs film (**ESI figure S1**). These lines arise from light interference in the porous film and as the thickness changes, different wavelength are successively reflected.<sup>27</sup>

The whole electrode was then introduced in a SEM and observed all along the z axis. In the **figure 2** are presented some SEM images of the TiO<sub>2</sub>-NTs films at different height of the electrode (the whole set of image can be seen in **ESI figure S2**). They clearly show the growth of the nanotubes from the initial state with small nanotubes of a few hundred nm at the top of the electrode to NTs with a length of several micrometers at the bottom. It should be noticed that for the shortest nanotubes, an initiation layer resulting from a pre-anodization step is still present. This first anodization and the removal of the primary nanotube layer is necessary to ensure a better adhesion of the nanotubes to the film and without this initial step, delaminating of the longer NTs is observed on the VLTE.<sup>28</sup> The length of the NTs at different positions on the electrode was measured and plotted in **figure 3.a**. It can be seen that this length increase from 780 to 5950 nm ± 200 nm and then is slightly reduced at the bottom of the nanotubes. The initial length is not zero since the electrolyte pumping starts 100 s after the beginning of the anodization. This duration is enough to form small NTs at the top of the electrode. The decrease of the length observed at the bottom of the electrode can be explained by the formation mechanism of the nanotubes which can be schematically described according to the following equations:



TiO<sub>2</sub> is formed electrochemically at the Ti surface while the nanotubular structure is achieved by its partial dissolution by the fluoride present in the electrolyte. The top of the nanotubes is then formed at the beginning of the anodization.

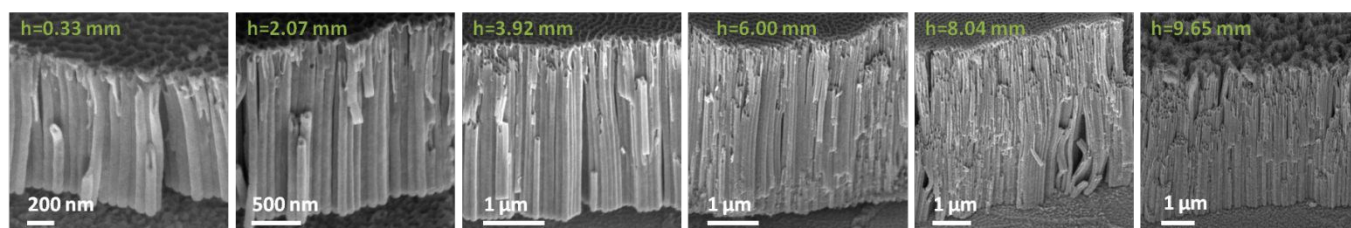


Figure 2 : SEM images of  $\text{TiO}_2$ -NTs observed at different height of the nanotubes (observed with a tilt angle of  $45^\circ$ ).

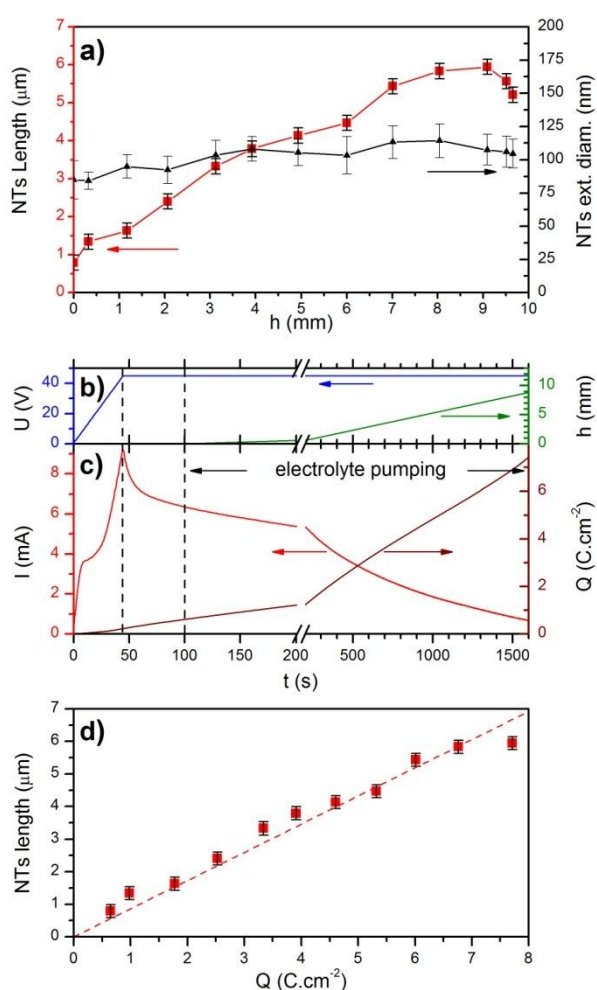


Figure 3: a) Length and diameter of the nanotubes as a function of the position from the top of the electrode determined by SEM. b) Anodization parameters: applied voltage and height of electrolyte pumped out as a function of time. c) Anodization current and calculated charge density evolution during the VLTE synthesis. d) Measured  $\text{TiO}_2$ -NTs length as a function of the calculated charge density ( $Q$ ) (correlation parameter estimated from linear regression:  $865 \text{ nm.C}^{-1}.\text{cm}^2$ ).

A too long exposure to the electrolyte results in the formation of a so-called “nanograss” layer at the top of the film.<sup>17</sup> This phenomenon results directly from a thinning of the nanotubes wall according to equation 2 and eventually the total

dissolution and collapse of the nanotube top, consequently the length does not increase continuously. This thinning of the NTs wall at the top can be observed in ESI **figure S3**: the SEM images of the top of the NTs film at different height (or anodization time) clearly show the transition from the initiation layer to the nanograss. In figure 3.a is also represented the values of NTs external diameter measured at their half height (diameters at the top and bottom of the nanotubes are presented in ESI **figure S4**). As observed in these synthesis conditions, the diameter has an average value of  $102 \pm 10 \text{ nm}$  and does not change significantly depending on the position of the NTs on the electrode.

The anodization data as a function of time are represented in figure 3.b and c. At the beginning, the applied voltage ( $U$ ) increases from 0 to 45 V this is accompanied by an increase of the current ( $I$ ) that reaches a maximum and slowly decrease when the potential stabilized to 45 V. It should be noticed that the current tends to 0 in our case since less surface is exposed, while for classical anodization the current reaches a plateau when an equilibrium between oxide formation and dissolution is reached (eq. 1&2). According to equation 1 the quantity of  $\text{TiO}_2$  formed during the anodization should be proportional to the charge transferred. In order to correlate this value with the length of the  $\text{TiO}_2$  nanotubes, we used the VLTE anodization data (**figure 3.b**) to determine the charge density transferred at each position of the electrode: First, the height of electrolyte pumped out as a function of time,  $h(t)$ , can be calculated from the flow imposed by the pump ( $f_p$ ) according to: (pump starts at  $t=100 \text{ s}$ ; for  $t < 100 \text{ s}$ ,  $h(t)=0$ )

$$h(t) = \frac{f_p(t-100)}{K} \quad (3)$$

The constant ( $K$ ) depends on the geometry of the container (its horizontal section) and correspond to the volume needed to change the height of 1 mm. In our case, the cell is a cylinder with a diameter of 7 cm and  $K=3.848 \text{ mL.mm}^{-1}$ . The value of  $h(t)$ , represented in figure 3.b (green curve) can be used to determine the surface of the electrode in contact with the electrolyte at any time. Knowing the anodization current from the synthesis data  $I(t)$  the charge used for the nanotube synthesis as a function of time and consequently each position of the electrode, can be calculated by the following integral:



$$Q(t) = \int_0^t \frac{I(t)}{W(L-h(t))} dt \quad (4)$$

with  $W$  and  $L$  the width and the length of the electrode. Then, the evolution between the nanotube length and the charge density can be represented (**figure 3.c**). Excluding the area where the nanograss is formed (*i.e.*  $h > 9.1$  mm or  $Q > 7.7$  C.cm<sup>-2</sup>), this evolution is linear with a growing ratio of 865 nm.C<sup>-1</sup>.cm<sup>2</sup>.

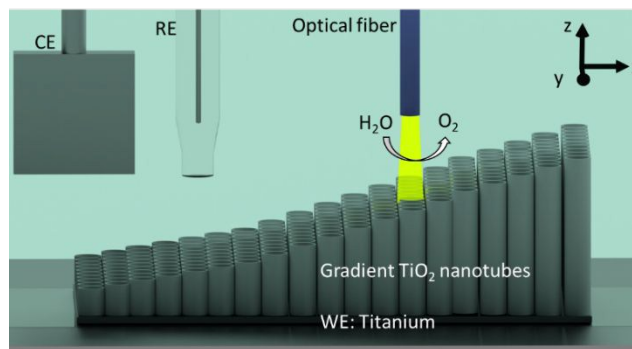


Figure 4: Scheme of the setup with the optical fiber scanning the gradient of TiO<sub>2</sub>-NTs during the SPECM experiment.

This confirms, on a single electrode, that accordingly with equation 1, the NTs length is proportional to the quantity of TiO<sub>2</sub> formed electrochemically. The length of the nanotubes in the VLTE can thus be estimated by knowing the total charge transferred at each position of the electrode for a given set of synthesis conditions.

## SPECM mapping

The VLTE electrode was fixed horizontally on a glass slide and then a cell made in PDMS was built around the sample. The SPECM experiment was run in a three electrodes configuration. A platinum mesh was used as the counter electrode and a Ag/AgCl (NaCl 3 M) as the reference electrode. The VLTE was the working electrode and its potential was set at 0.6 V vs Ag/AgCl. The sample was irradiated through an optical fiber with a numerical aperture of 0.22 and a core diameter of 200 μm. The light source was a mercury-xenon lamp (LC8 from Hamamatsu) providing a spectrum centered at 365 nm. The optical fiber was moved along  $xy$  axes at a scan rate of 400 μm.s<sup>-1</sup>, with steps every 40 μm each 0.1 s,  $z$ , the distance between the tip and the surface was constant (20 μm) during the measurement. When the UV source was turned on, the optical fiber illuminated locally the TiO<sub>2</sub>-NTs, and the current was simultaneously recorded as a function of the optical fiber position. This current corresponds to the local photoelectrochemical oxidation of water, which happens only below the light spot. With this system, a 2D image of TiO<sub>2</sub> nanotube gradient was obtained on an area of 10\*2 mm<sup>2</sup>, located in the middle of the electrode, first in the dark then under illumination with UV light (**figure 5.a**).

In the dark, the current has a residual value below 6.5 μA. Under UV light irradiation, an increase of the current clearly appears on the sample even for short nanotubes. This current

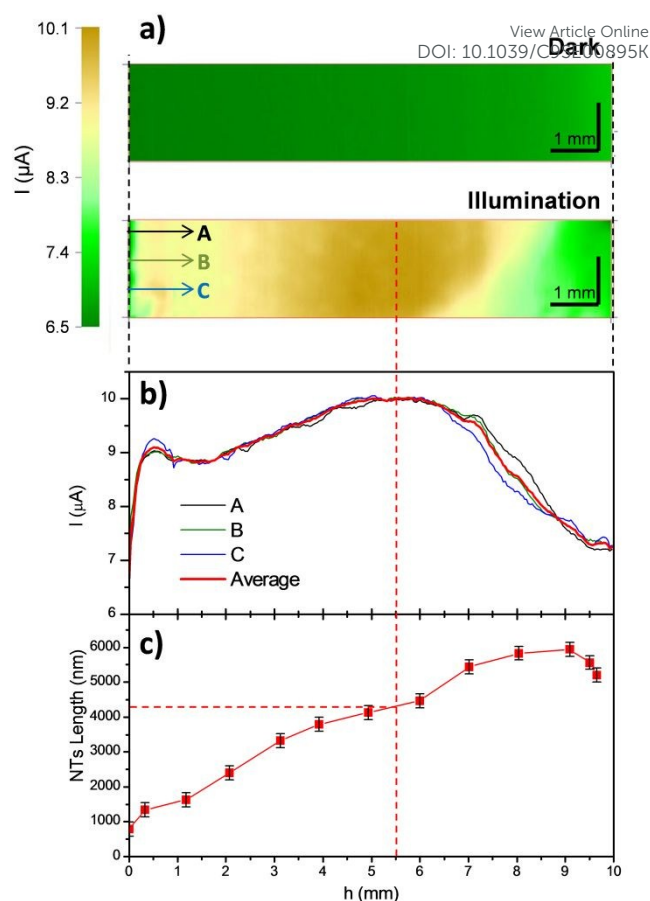


Figure 5: a) SPECM results in the dark and under illumination at  $\lambda = 365$  nm, b) Photocurrent profile at 3 positions and c) corresponding NTs length for the same VLTE.

increases until a maximum located approximately in the center of the electrode. Then, for the longer nanotubes, the photocurrent decreases. In figure 5.b are represented the photocurrent evolutions on three positions of the electrode and their average. The photocurrent appears for short nanotubes and reaches a local maximum at 0.5 mm from the top of the electrode. This local maximum, might be attributed to the partial contribution of the dense underlying TiO<sub>2</sub> layer located at the interface between the NTs and Ti substrate.<sup>6</sup> With longer nanotubes, the contribution of this dense layer is reduced since less light can reach it and mainly the NTs contribute to the photocurrent. After this local maximum, the photocurrent increases with the length of the NTs until a maximum of 10.1 μA at 5.5 mm from the top of the electrode; a position for which TiO<sub>2</sub>-NTs have a length of  $4.3 \pm 0.2$  μm. The length corresponding to this maximal photocurrent is coherent with measurements performed for nanotubes of different lengths, synthesized by a classical method. As detailed in supplementary information (ESI **figure S6**), TiO<sub>2</sub>-NTs films with different lengths, were tested in a normal 3 electrodes PEC setup. The highest photocurrent and yield were measured for NTs with a length of approximately 4 μm. This value is also in agreement with the optimal thickness of NTs film reported, by other teams, to be between 4 and 6 μm in the case of photo-(electro)catalytic applications.<sup>29,30</sup> This maximum of efficiency

for this length is explained by a balance between two properties governing the photocurrent generation: (i) a good light absorption, resulting in high number of  $e^-/h^+$  pairs generated which increases with the thickness and (ii) the efficient transport of the electron to the back contact (the Ti foil). The latter is limited by the diffusion of electrons in  $\text{TiO}_2$  and will then be reduced for thick nanotubes films.<sup>6,9</sup>

To determine the reliability of our approach combining variable length nanotubes synthesis and SPECM measurements, we compared our results with a reference  $\text{TiO}_2$ -NTs electrode. For this, nanotubes were grown in the same electrolyte and the charge transferred was limited to  $5 \text{ C.cm}^{-2}$ , resulting in a titanium foil covered with NTs having a length of  $4050 \pm 110 \text{ nm}$ . The external quantum efficiency (EQE) of this electrode was then measured (data are in **figure S7**). EQE represents the ratio between the quantity of electron collected and the number of incident photon at a given wavelength according to:

$$EQE(\lambda) = \frac{h \cdot c}{e} \left( \frac{j_{ph}(\lambda)}{P(\lambda) \cdot \lambda} \right) \quad (5)$$

With  $j_{ph}(\lambda)$  and  $P(\lambda)$  are the measured photocurrent and the incident light power density at a given wavelength  $\lambda$ , respectively. For the reference electrode an EQE value of 0.15 was obtained at 365 nm which is the central wavelength of the UV light source used in SPECM setting. The same calculation can be done for the SPECM system knowing the irradiation power at the optical fiber exit ( $115 \pm 50 \text{ } \mu\text{W}$ ). For NTs having a length of 4000 nm the measured photocurrent triggered by this irradiation is  $3.5 \text{ } \mu\text{A}$ . By applying equation 5, an EQE of  $0.15 \pm 0.06$  is obtained. This value is in good agreement with the EQE obtained at 365 nm for the reference sample, confirming the good response of the VLTE electrode even with the localized spot of the SPECM system (estimated spot diameter  $215 \pm 50 \text{ } \mu\text{m}$ ). The high uncertainty is explained by the difficulty to measure the power at the fiber output.

## Defect identification with SPECM

In **figure 6** is presented the SPECM mapping of a part of a second VLTE electrode. For this electrode, the evolution of nanotubes length as a function of the anodization charge was calculated according the same protocol as earlier, and the growing factor of  $850 \text{ nm.C}^{-1}.\text{cm}^2$  is consistent with the first sample. The calculation and data for this sample are presented in **figure S12**. On the photocurrent mapping, lines with lower photocurrent can be observed on the left of the image which corresponds to the bottom of the electrode. Their positions correspond to scratches that were done on one side of the electrode surface. As observed by SEM in **figure 6.b**, these scratches are  $10 \text{ } \mu\text{m}$  in width. Even if the optical fiber aperture is larger, the good spatial and electrochemical resolution of the SPECM, allows localizing these stripes. Similarly, a small round area can be observed in the center of the mapping image. Its position perfectly matches with a small punch that was done with an needle on the VLTE sample that can be observed optically in **image 6.c**.

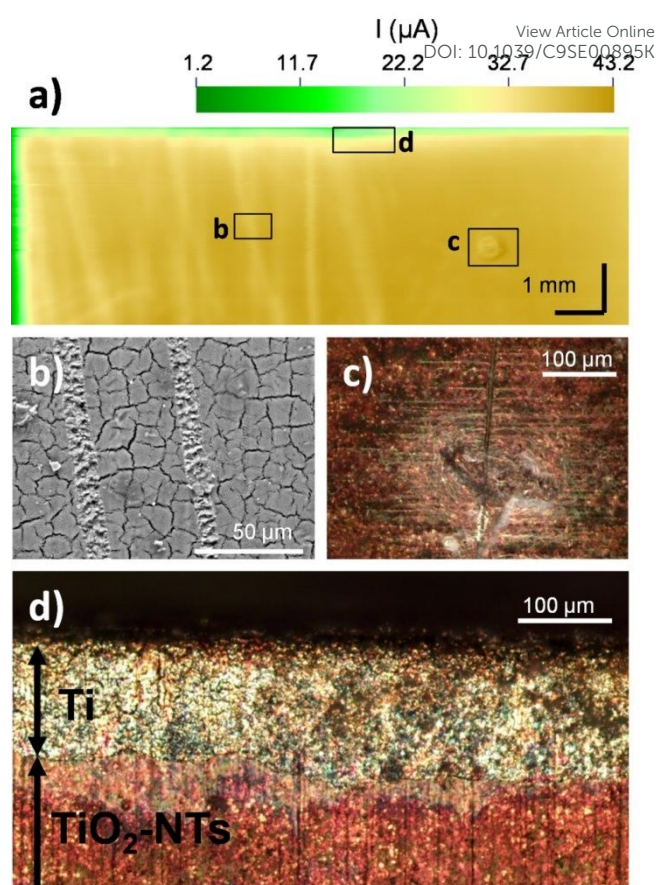


Figure 6: a) SPECM mapping of a second VLTE sample. b) SEM images of scratches made at the bottom of the nanotubes. c) and d), dark field optical images of a punching on the  $\text{TiO}_2$ -NTs electrode and of the side of the electrode.

The mapping of this VLTE surface was done on the side of the titanium foil and small strip with low photocurrent can be observed at the top and the left of the figure 6.a. This observation can be related to side effect phenomenon occurring during the growth of the nanotubes film. This can be optically related to the observation of **figure 6.d**: on this dark field image of the surface, at the top edge of the electrode, the  $\text{TiO}_2$ -NTs film appears in red and a strip of approximately  $100 \text{ } \mu\text{m}$  non covered with nanotubes appears on the side of the electrode in grey. This can be explained by a peeling of the nanotubes film on the side of the electrode during the synthesis or rinsing/annealing step. This side effect was also observed for other samples (example of dark field images in **Figure S5**).

Besides confirming the reproducibility of the VLTE electrode synthesis, the observation of this second sample allows to highlight the good resolution and the potential application of the SPECM method to detect point defects in electrodes for PEC applications.

## Conclusions

In this work we report a simple and reproducible synthesis method of aligned  $\text{TiO}_2$ -NTs electrode on which the length of the nanotubes can be tuned along one direction. By changing

the contact time between the electrolyte and the titanium substrate, NTs having a length ranging from a few hundred nm up to few  $\mu\text{m}$  can be grown on a single electrode. Furthermore, by this approach the diameter of the nanotubes does not change significantly and this type of electrode allows local studies of the influence of the NTs length independently of others parameters.

In order to measure the performance of these original samples with a variable thickness of photoactive material, we used by SPECIM in order to study the influence of the nanotubes length on the generated photocurrent for water splitting reaction. The mapping image revealed significant photocurrent change in the direction of the length gradient while a good homogeneity of the photocurrent appears in the lateral direction. The photocurrent profile indicates a maximum for nanotubes having a length of 4300 nm; a value which is consistent with previously reported studies. This approach combining gradient synthesis and SPECIM measurement can be used to measure quickly the optimal value of a parameter while limiting the synthesis time by doing all the test locally on a single electrode.

Furthermore the SPECIM measurements present an excellent spatial and electrochemical resolution that could allows to detect defects in photo-electrochemical films in the perspective of electrodes diagnostic. We believe this resolution can further be improved by playing on the electrochemical parameters and the aperture of the optical fiber.

## Conflicts of interest

There are no conflicts to declare.

## Acknowledgements

FG is grateful to CNRS for funding is PhD research through the ANR BAGETE (ANR-16-CE05-0001-01). Thierry Dintzer and the SEM-CRO Platform are acknowledged for SEM images.

## References

- 1 N. S. Lewis, *Science*, 2016, **351**, aad1920.
- 2 S. I. Seok, M. Grätzel and N.-G. Park, *Small*, 2018, **14**, 1704177.
- 3 Y. Yang, S. Niu, D. Han, T. Liu, G. Wang and Y. Li, *Adv. Energy Mater.*, 2017, **7**, 1700555.
- 4 K. Sivula and R. van de Krol, *Nat. Rev. Mater.*, 2016, **1**, 15010.
- 5 F. E. Osterloh, *Chem Soc Rev*, 2013, **42**, 2294–2320.
- 6 P. Schmuki, K. Lee and A. Mazare, *Chem. Rev.*, 2014, **114**, 9385–9454.
- 7 L. M. Peter, *Electroanalysis*, 2015, **27**, 864–871.
- 8 D. Klotz, D. A. Grave and A. Rothschild, *Phys Chem Chem Phys*, 2017, **19**, 20383–20392.
- 9 K. Takanabe, *ACS Catal.*, 2017, **7**, 8006–8022.
- 10 N. S. Lewis, M. G. Walter, E. L. Warren, J. R. McKone, S. W. Boettcher, Q. Mi and E. A. Santori, *Chem. Rev.*, 2010, **110**, 6446–6473.

- 11 K. Sliozberg, H. S. Stein, C. Khare, B. A. Parkinson, A. Ludwig and W. Schuhmann, *ACS Appl. Mater. Interfaces*, 2015, **7**, 4883–4889.
- 12 K. Sliozberg, D. Schäfer, T. Erichsen, R. Meyer, C. Khare, A. Ludwig and W. Schuhmann, *ChemSusChem*, 2015, n/a–n/a.
- 13 P. N. Anunson, G. R. Winkler, J. R. Winkler, B. A. Parkinson and J. D. Schuttlefield Christus, *J. Chem. Educ.*, 2013, **90**, 1333–1340.
- 14 G. Loget, S. So, R. Hahn and P. Schmuki, *J Mater Chem A*, 2014, **2**, 17740–17745.
- 15 G. Loget and P. Schmuki, *Langmuir*, 2014, **30**, 15356–15363.
- 16 P. Mu, Y. Li, Y. Zhang, Y. Yang, R. Hu, X. Zhao, A. Huang, R. Zhang, X. Liu, Q. Huang and C. Lin, *ACS Biomater. Sci. Eng.*, 2018, **4**, 2804–2814.
- 17 P. Roy, S. Berger and P. Schmuki, *Angew. Chem. Int. Ed.*, 2011, **50**, 2904–2939.
- 18 N. Casillas, *J. Electrochem. Soc.*, 1995, **142**, L16.
- 19 J. Lee, H. Ye, S. Pan and A. J. Bard, *Anal. Chem.*, 2008, **80**, 7445–7450.
- 20 R. Gutkowsky, C. Khare, F. Conzuelo, Y. U. Kayran, A. Ludwig and W. Schuhmann, *Energy Environ. Sci.*, 2017, **10**, 1213–1221.
- 21 H. Ye, H. S. Park and A. J. Bard, *J. Phys. Chem. C*, 2011, **115**, 12464–12470.
- 22 G. Wittstock, S. Rastgar and S. Scarabino, *Curr. Opin. Electrochem.*, 2019, **13**, 25–32.
- 23 V. Badets, G. Loget, P. Garrigue, N. Sojic and D. Zigah, *Electrochimica Acta*, 2016, **222**, 84–91.
- 24 K. C. Leonard, K. M. Nam, H. C. Lee, S. H. Kang, H. S. Park and A. J. Bard, *J. Phys. Chem. C*, 2013, **117**, 15901–15910.
- 25 J. S. Jang, K. Y. Yoon, X. Xiao, F.-R. F. Fan and A. J. Bard, *Chem. Mater.*, 2009, **21**, 4803–4810.
- 26 J.-H. Ni, C. J. Frandsen, L.-H. Chen, Y.-Y. Zhang, J. Khamwannah, G. He, T.-T. Tang and S. Jin, *Adv. Eng. Mater.*, 2013, **15**, 464–468.
- 27 T. Cottineau, H. Cachet, V. Keller and E. M. M. Sutter, *Phys. Chem. Chem. Phys.*, 2017, **19**, 31469–31478.
- 28 J. M. Macak, S. P. Albu and P. Schmuki, *Phys. Status Solidi RRL – Rapid Res. Lett.*, 2007, **1**, 181–183.
- 29 C. B. Marien, T. Cottineau, D. Robert and P. Drogui, *Appl. Catal. B Environ.*, 2016, **194**, 1–6.
- 30 X. Zhang, K. Huo, L. Hu, Z. Wu and P. K. Chu, *J. Am. Ceram. Soc.*, 2010, **93**, 2771–2778.





Table of Content Entry for:

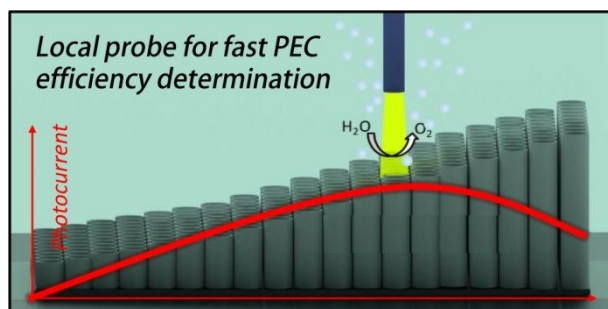
## Electrosynthesis of gradient $\text{TiO}_2$ nanotubes and rapid screening using Scanning PhotoElectroChemical Microscopy

Florian Gelb,<sup>a</sup> Yu-Chien Chueh,<sup>b</sup> Neso Sojic,<sup>b</sup> Valérie Keller,<sup>a</sup> Dodzi Zigah<sup>b</sup> and Thomas Cottineau<sup>\*a</sup>

<sup>a</sup> CNRS, Univ. Strasbourg, Institut de Chimie et Procédés pour l'Energie, l'Environnement et la Santé, UMR 7515, 25 rue Becquerel, 67087 Strasbourg, France.

<sup>b</sup> Univ. Bordeaux, CNRS, Bordeaux INP, Institut des Sciences Moleculaires, UMR5255, 16 Avenue Pey-Berland, 33400 Talence, France

\* Corresponding author: cottineau@unistra.fr



Electrodes of  $\text{TiO}_2$ -nanotubes with a gradient of length were synthesized by a simple anodization method and analyzed locally by scanning PhotoElectroChemical Microscopy.